ASSESSMENT OF THE LEAF AREA INDEX FOR SUMMER BARLEY FROM FIELD SPECTRORADIOMETER AND HYMAP IMAGE DATA USING THE PROSPECT + SAIL MODELS

Michael Vohland[1], Thomas Jarmer[2] and Sebastian Mader[3]

1. University of Trier, Remote Sensing and Geoinformatics, D-54286 Trier, Germany; vohland@uni-trier.de
2. Free University of Berlin, Remote Sensing and Geoinformatics, D-12249 Berlin, Germany; jarmer@geog.fu-berlin.de
3. University of Trier, Remote Sensing Department, D-54286 Trier, Germany; made6101@uni-trier.de

ABSTRACT

The estimation of the LAI plays an important role in many vegetation related issues. In this study, LAI assessment from remote sensing data was performed for summer barley stands (n = 16). For the study time at the end of May, ground truth LAI data and both field spectroradiometer (ASD FieldSpec II) and airborne hyperspectral image data (HyMap) were available. For reasons of a more general applicability with less restrictions, a physical approach coupling the radiative transfer models PROSPECT and SAIL was preferred to a purely empirical approach. Some constraints were introduced for the PROSAIL inversion; the most important was the coupling of the equivalent water thickness and the dry matter content of leaves. In the following, the model inversion was performed using the Nelder Mead Simplex method for the spectroradiometer measurements, synthetic HyMap spectra (generated by resampling the field spectra) and the HyMap image data. For the latter, pixel values were extracted near the field-measured GPS-coordinates using a spatial subset of 3 × 3 pixels. In fact, for nearly all sub-plots spectra could be extracted that matched the spectroradiometer data and did not reveal spatial scaling effects or deficiencies of radiometric preprocessing. The accuracies of LAI estimation were very high for the spectroradiometer data ($r^2 = 0.90$), but diminished slightly for the synthetic HyMap data ($r^2 = 0.87$). For the image spectra, LAI estimates were still satisfying with r^2 equalling 0.80.

INTRODUCTION

The leaf area index (LAI) is referred to as essential structural or biophysical parameter of vegetation canopies that is specifically linked with other canopy variables (e.g., ground coverage, above-ground biomass, crop yield) and therefore an appropriate indicator of crop growth during the complete phenological cycle. Thus, in terms of precision agriculture, the LAI assessment can be useful for the detection of growth anomalies. Furthermore, it forms an important input for many ecological, hydrological or climatological modelling approaches; e.g., for a model-based reconstruction of the complex interaction between soil, vegetation and atmosphere, a precise LAI estimation is obligatory.

In the past, many studies have been carried out for retrieving LAI from remote sensing data. Compared to the classical multispectral approaches, hyperspectral remote sensing provides new potentials for vegetation analysis and LAI assessment (i, ii). For instance, a couple of new hyperspectral indices have been designed (e.g., iii), but their application suffers from the fact that they are per se not transferable in space and time. Thus, the application of physical algorithms is desirable for a more powerful estimation approach being less restricted to the calibration data.

Physical approaches rely on inverting canopy reflectance models that allow a process-related insight in the interaction between vegetation canopy and incoming solar radiation. In this

study, the PROSPECT and SAIL models were coupled, and their inversion was performed for summer barley plots investigated in May 2005. In literature, PROSAIL has been applied in a whole lot of studies for agricultural crops, but nevertheless, investigations of the model performance on synthetic data are in greater numbers than studies using real data (iv). For the summer barley plots investigated here, model inversion for LAI assessment has been applied to real data both measured by the airborne HyMap sensor and acquired by a field spectroradiometer (ASD FieldSpec II) during or near the HyMap overflight. Thus, radiometric preprocessing and spatial scaling effects are issues of concern. Furthermore, the ASD FieldSpec II data were resampled to synthetic HyMap data to investigate effects solely induced by the spectral resolution without spatial implications. LAI ground truth data were surveyed destructively to enable the validation of the model performance on the different data sets.

METHODS

Study site and field data

The study site is located near Newel in the Eifel region (Rhineland-Palatinate, Germany, Figure 1). Here, two fields that were cropped with summer barley in 2005 were selected for further investigation.
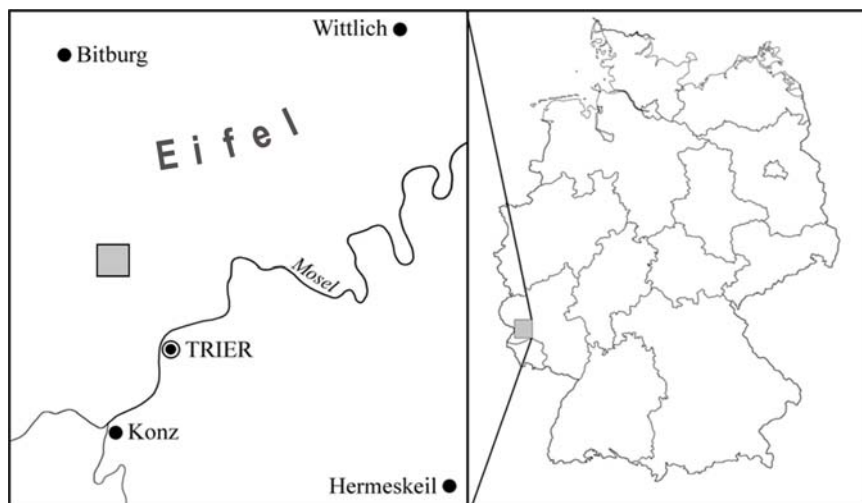

Figure 1: Location of the study site (Rhineland-Palatinate, Germany).

The field work was carried out at the 27th and 28th of May; at these dates, the summer barley showed clear differences in terms of phenology (partly still tillering, partly clearly pronounced stem elongation). For altogether 16 sub-plots with a size of 50 × 50 cm², integrative in situ reflectance measurements were performed using an ASD FieldSpec II instrument that provides spectra with an increment of 1 nm from 350 up to 2500 nm. The spectral readings were taken with nadir view in the principal plane; absolute bi-directional reflectances were obtained by normalizing the readings with a certified Spectralon panel. The exact position was located for each sub-plot using a differential GPS. After the spectra collection, the above-ground plant material of the sub-plots was harvested. In the laboratory, the fractions of green and yellow leaves were separated for each sample and both the total and green LAI were determined by scanning the leaves with a LI-COR 3000C leaf area meter.

The preprocessing of the field spectra consisted of a third order-polynomial Savitzky-Golay filtering (frame size 21 nm); furthermore, the reflectance values of noisy bands (< 400 nm, > 2400 nm) and in the major parts of the atmospheric water vapour absorption (1360-1420 nm, 1790-1940 nm) were eliminated. Thus, the spectral bands were reduced from the original number of 2151 to 1789 with a width of 1 nm. In the following, these spectra were resampled to the spectral resolution of the HyMap sensor. As nine HyMap bands are located in the spectral regions eliminated, the final synthetic HyMap spectra provided are made up by 117 spectral bands instead of the original number of 126.

HyMap image data

A data set of the HyMap airborne imaging sensor was acquired on the 28th of May (acquisition time: 9:01:20 UTC) during the HyEurope 2005 campaign. In the delivered data, the spectral range from 434 to 2486.5 nm (central wavelengths of the first and last band) is covered by 126 bands with bandwidths ranging from 12.9 to 21.3 nm. The ground resolution realized in the overflight was approximately 5 m.

As the flight path was from the Northwest southeastwards (flight heading 325°), an across-track illumination correction was performed for a spatial subset excluding forested areas. In the following, the FLAASH (Fast Line of-sight Atmospheric Analysis of Spectral Hypercubes) module of ENVI™, based on the MODTRAN4 radiation code (v), was used for the atmospheric correction (Table 1). A parametric geometric correction was performed using the PARGE™ software (vi) by integrating a high resolution digital elevation model, GPS ground control points and flight navigation data provided with the HyMap data.

For a consistent analysis, the corrected image file was adapted to the synthetic HyMap data by eliminating the spectral bands mentioned above. Furthermore, two other noisy bands nearby the 1.4 µm water vapour absorption feature (1421.7 nm, 1435.9 nm) were removed. Thus, the final image product resulting from the different steps of preprocessing provided geocoded reflectance values in altogether 115 spectral bands.

Table 1: FLAASH parameters for the atmospheric correction.

Atmospheric model	Aerosol model	Estimated horizontal visibility	Average water amount
Mid-Latitude Summer	rural	20.6 km	2.305 g cm^{-2}

The PROSAIL modelling approach

For this investigation, the PROSPECT model describing the optical properties of plant leaves (vii) has been coupled with the SAIL model (viii), a 1 D turbid medium radiative transfer model and therefore suited for the study of homogeneous vegetation canopies. The full inversion of PROSAIL from spectral measurements is enabled by a controllable number of parameters introduced in the model (Figure 2, Table 2). By model inversion, the estimates for the stand variables are obtained by an iterative minimization of the merit function (Figure 2); thus, the best fit between observed data (canopy reflectances measured by the FieldSpec II or HyMap instrument) and predictions based on the PROSAIL model will provide the final approximation of the canopy variables. However, several sets of parameters correspond with spectral signatures similarly, which is the main reason for the ill-posed problem of the model inversion (ix).
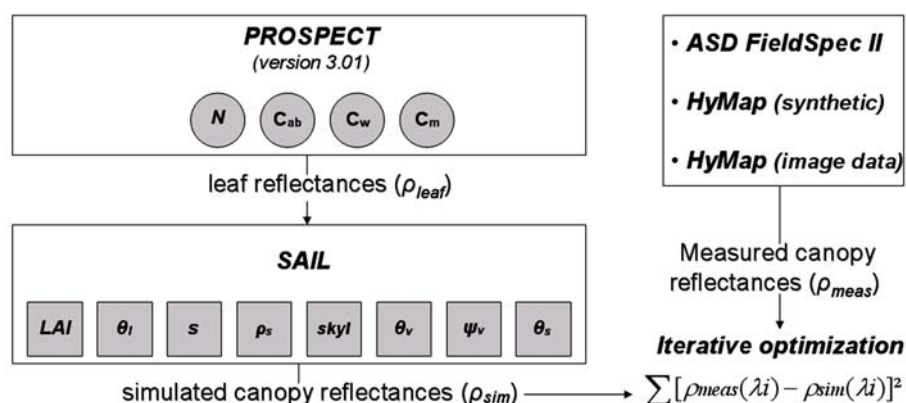

Figure 2: PROSAIL inversion from spectral measurements of the test plots.

Table 2: Model parameters and constraints for the model inversion.

Parameter	Definition	Range of variation
N	leaf structure parameter	fixed to 1.3
C_{ab} [µg cm^{-2}][a]	chlorophylls a+b	1 – 100
C_w [g cm^{-2}][a]	equivalent water thickness	0.006 – 0.05[c]
C_m [g cm^{-2}][a]	dry matter content	0.0015 – 0.0125[c]
LAI	leaf area index	0.01 - 9.0
θ_l [°]	mean leaf inclination angle	20 - 70
s [b]	hot spot size parameter	fixed to 0.1
ρ_s	soil spectral reflectance	known (fixed)
skyl	diffuse illumination fraction	fixed to 0.01
θ_v [°]	zenith viewing angle	0°
ψ_v [°]	relative viewing azimuth	0°
θ_s [°]	zenith solar angle	known

[a] per leaf area
[b] hot spot-modification introduced by Kuusk (**x**); SAILH
[c] tied together

Plausible constraints by integrating prior information are helpful to reduce the ill-posed nature of model inversion (xi). Thus, based on the findings of other studies (ix, xii, xiii), some model parameters were fixed (N, s and skyl; Table 2). To define ρ_s, soil samples were taken in the field to identify a typical background soil reflectance that was used for the inversion of all samples. Furthermore, we extended the inversion routine by coupling EWT and leaf dry mass, and introduced all plausible combinations of C_m (range: 0.0015-0.0125 g cm^{-2}) and C_w in a ratio of 1:4. This constraint is based on the fact, that the foliage moisture content (FMC [%] = ($C_w \times C_m^{-1}$) × 100; amount of water per unit of dry matter) usually amounts about 400 % for fresh plant material; a detailed discussion of coupling C_m and C_w can be found in xiii.

The LAI and the other unknown parameters (Cab, Cw, Cm, θ_l) were obtained from the different sets of reflectance data (Figure 2) using the Nelder-Mead Simplex method for minimization. One deficit of this method is its sensitivity to the initial parameter values that was reduced by iterative minimization with repeated recovering of the initial values with previous results.

The spectra extraction from the HyMap data was performed by means of the GPS coordinates measured in the field. However, these coordinates refer to the centre of 50 × 50 cm² plots, and – due to unavoidable inaccuracies of image geocodation and differential GPS measurements – it is questionable whether the pixel at the nearest neighbour position is really the right and corresponding one. Thus, we used a window of 3 × 3 pixels that was centred at the GPS-defined image coordinates to extract altogether three alternative spectral samples: a first incorporating the spectra at the nearest neighbour positions, a second made up by the mean values of all nine pixels, and finally a third set by extracting the pixels fitting best to the field measured spectra. For all sets, LAI was estimated by means of PROSAIL inversion.

RESULTS & DISCUSSION

LAI assessment from ASD FieldSpec II and synthetic HyMap data

In the PROSAIL inversion from the ASD readings, a good fit was achieved between the measured spectra and the spectra reconstructed using the found parameter values. The RMSE – in terms of absolute reflectances ($RMSE_\rho$) – varied between 0.0094 and 0.0185; the mean $RMSE_\rho$ for all 16 plots equalled 0.0138.
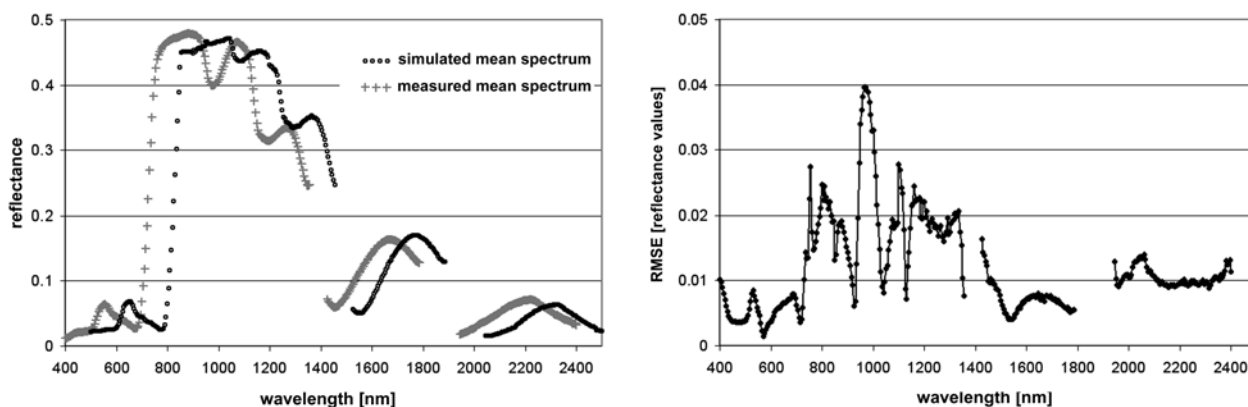
Figure 3: Measured (ASD FieldSpec II) vs. PROSAIL reconstructed spectra: Mean spectra and mean $RMSE_\rho$ (n = 16) (for demonstration purposes, the "simulated mean spectrum" has been shifted in the x-direction by 100 nm).

As function of wavelength (Figure 3), the mean $RMSE_\rho$ is almost stable and small. Only one peak ($RMSE_\rho$ about 0.04) is noticeable, that is to be found at the 980 nm-water absorption feature, whereas the second clearly pronounced water absorption feature near 1200 nm is reconstructed accurately. Furthermore, the shoulder in the simulated red-edge region near 750 nm seems to be too sharp, which is referred to in other studies and presumably induced by the specific absorption coefficients of the original PROSPECT version (xiii, xiv).

The inversion procedure provided LAI estimates highly correlated with both total and green LAI values (Figure 4). In terms of RMSE, the estimation accuracy is higher for the fraction of green leaves. For both samples, there is an overall tendency of overestimating low and – even more clearly – underestimating high LAI values. However, this trend is diminished for the green LAI with estimates grouped around the 1:1-line closely. This finding is plausible, as PROSAIL does not take into account the presence of senescent leaves, which will induce estimation inaccuracies at maturity and senescence stages (iii). As our study time was end of May, this effect plays a minor role for the plots investigated here.
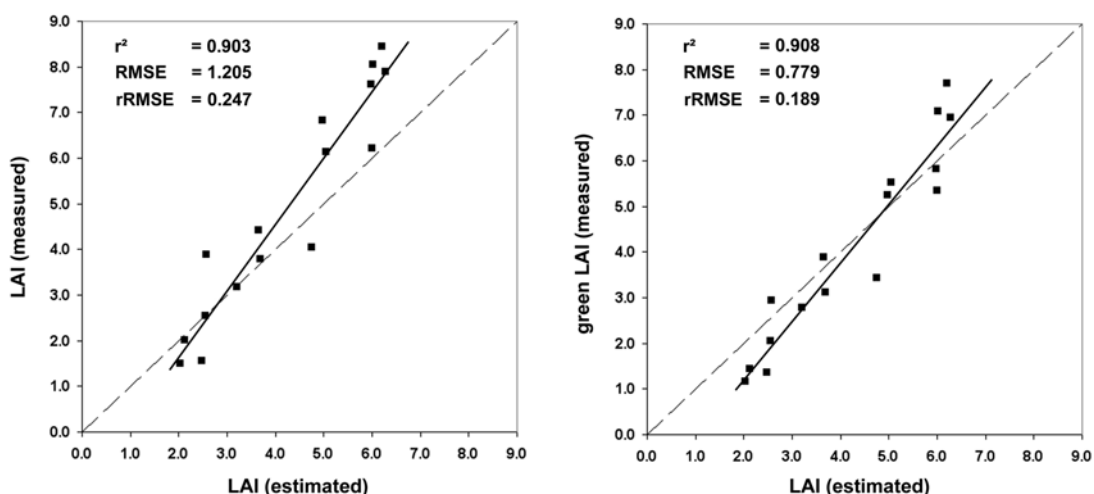

Figure 4: Coefficients of determination [a], RMSE and rRMSE [b] obtained for total LAI and green LAI from spectroradiometer measurements (n = 16) ([a]correlations statistically significant with α < 0.01; [b]relative RMSE, defined as RMSE × mean LAI[-1]).

In the next step, the synthetic HyMap data were introduced in the PROSAIL inversion procedure. Again, a very good spectra reconstruction was achieved ($RMSE_\rho$= 0.0143). Compared to the original spectroradiometer spectra, the parameter estimation accuracies slightly diminished for the green LAI, whereas for the total LAI at least the RMSE kept stable (Table 3).

Furthermore, the LAI estimates based on the synthetic spectra (117 spectral bands) were highly correlated with the estimates provided by inverting the full spectra (r = 0.99); the absolute RMSE between both samples equalled 0.249.

Table 3: Estimation accuracies for LAI by PROSAIL using synthetic HyMap spectra (n = 16).

	r²	RMSE	rRMSE
total LAI	0.869 [b]	1.171	0.240
green LAI	0.875 [b]	0.885	0.215

[a] correlation statistically significant with α < 0.01

LAI assessment from HyMap image data

In a first analysis, the different samples of image spectra were compared to the field measured spectra. The reconstruction of the field spectra by those pixels that provided the best fit resulted in an overall $RMSE_\rho$ of 0.0180 (n = 16). Nevertheless, for three sub-plots the results of this procedure were only moderate, as the $RMSE_\rho$ identified were more than 0.020 (maximum 0.0352). For illustration, we plotted both the mean spectra (as measured in the field and extracted from the HyMap data) and the residuals averaged for all sub-plots (Figure 5) as function of wavelength. The maximum residuals are to be found in the red-edge region, the first water absorption feature at 980 nm and in the spectral bands preceding the absorption feature at 1400 nm. However, residuals are rather small, and clear deficiencies of radiometric preprocessing are not evident.
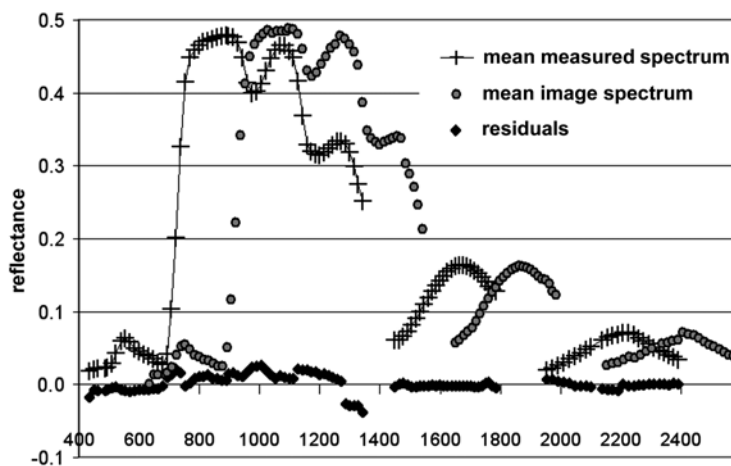

Figure 5: Field measured spectra (ASD FieldSpec II, resampled to HyMap bands) versus HyMap image spectra: Mean course and residuals (averaged for n = 16) (for demonstration purposes, the "mean image spectrum" has been shifted in the x-direction by 200 nm).

The alternative approaches to select image spectra were much less promising: extracting the nearest neighbour pixels provided an overall $RMSE_\rho$ of 0.0486, and the sample made up by the mean of the selected nine pixels resulted in an $RMSE_\rho$ of 0.0301. These error terms are consistent with the findings of the field work, as canopy architecture and development stage clearly varied in space and complicated the identification of more or less homogeneous sub-plots for LAI and spectra collection. Nevertheless, the successful identification of image pixels matching field spectra indicates that scaling effects seem to be of minor relevance for the studied samples.

Using the identified set of pixel values matching the field spectra, the results of LAI estimation worsened slightly compared to the inversion of both spectroradiometer and synthetic HyMap data, but still proved to be satisfying (Figure 6). For the HyMap data, LAI estimates for the

green LAI were not more accurate than for the total LAI. Spectra reconstruction by PROSAIL again succeeded with an $RMSE_\rho$ of 0.0176.
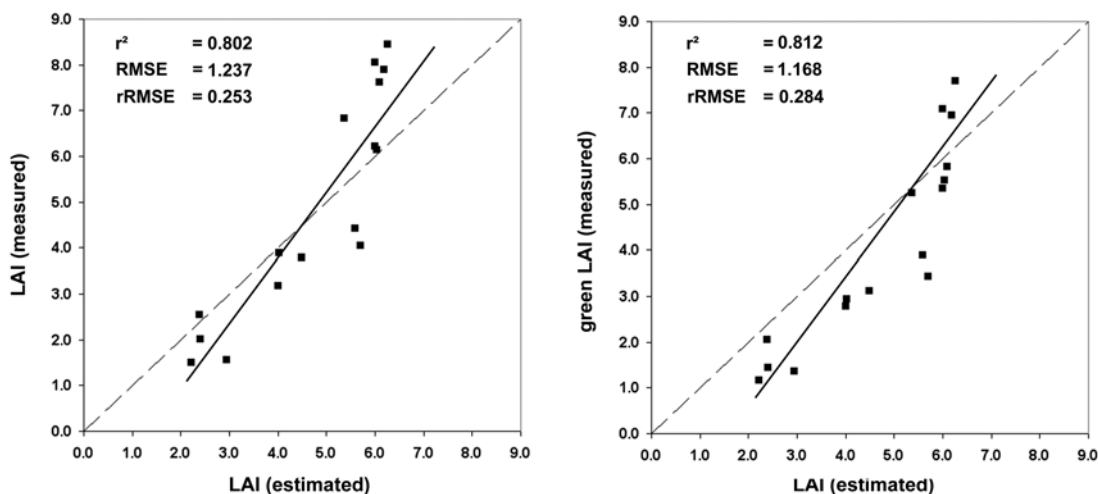

Figure 6: Coefficients of determination [a], RMSE and rRMSE obtained for total LAI and green LAI (n = 16) from HyMap image data ([a]correlations statistically significant with α < 0.01).

As to be expected, estimation results on the other spectral samples extracted from the Hy-Map data were poor; for the total LAI, r² differed from 0.192 (mean spectra) to 0.204 (nearest neighbour pixels) and RMSE equalled 2.131 and 2.165 respectively; for the green LAI, r² was 0.208 and 0.219 respectively, RMSE equalled 2.104 and 2.244.

CONCLUSIONS

In literature, only a limited number of studies using real data of crop stands (reflectance measurements and associated ground data) for evaluating the performance of PROSAIL can be found (e.g., iv, xii, xv). Nevertheless, the LAI estimates obtained in this study document the estimation power of PROSAIL after introducing some basic constraints (e.g., coupling equivalent water thickness and leaf dry matter content). Results were presumably favoured by the study time; for phenological reasons, inversion procedure was almost not affected by the presence of senescent plant material or spikes.

Spatial scaling effects induced by the different remote sensors' ground resolutions were not studied systematically, as the set of available field spectroradiometer measurements was too limited. However, the pixelwise analysis of the HyMap data provided a set of spectra matching the field measurements; thus, spatial scaling effects appeared to be of minor relevance for this data sample. Accordingly, the loss of LAI estimation accuracy from spectroradiometer data to HyMap image data was only moderate and results kept satisfying.

The HyMap data were subjected to a standard preprocessing neglecting terrain-induced illumination effects and sensor recalibration. Nevertheless, error terms clearly resulting from the radiometric preprocessing were not evident.

ACKNOWLEDGEMENTS

REFERENCES

i   Liang S, 2004. Quantitative Remote Sensing of Land Surfaces (Wiley-Interscience), 534 pp.

ii   Thenkabail P S, E A Enclona, M S Ashton & B Van Der Meer, 2004. Accuracy assessments of hyperspectral waveband performance for vegetation analysis applications. Remote Sens. Environ., 91: 354-376

iii Haboudane D, J R Miller, E Pattey, P J Zarco-Tejada & I B Strachan, 2004. Hyperspectral vegetation indices and novel algorithms for predicting green LAI of crop canopies: Modeling and validation in the context of precision agriculture. Remote Sens. Environ., 90: 337-352

iv   Jacquemoud S, C Bacour, H Poilvé & J P Frangi, 2000. Comparison of four radiative transfer models to simulate plant canopies reflectance: Direct and inverse mode. Remote Sens. Environ., 74: 471-481

v   Matthew M W, S M Adler-Golden, A Berk, S C Richtsmeier, R Y Levine, L S Bernstein, P K Acharya, G P Anderson, G W Felde, M P Hoke, A Ratkowski, H-H Burke, R D Kaiser& D P Miller, 2000. Status of Atmospheric Correction Using a MODTRAN4-based Algorithm. In: Proc. SPIE 4049, 199-207

vi   Schläpfer D & R Richter, 2002. Geoatmospheric Processing of Airborne Imaging Spectrometer Data Part1: Parametric Orthorectification. Int. J. Rem. Sens., 23:2609-2630

vii Baret F & T Fourty, 1997. Estimation of leaf water content and specific leaf weight from reflectance and transmittance. Agronomie, 17: 455-464

viii Verhoef W, 1984. Light scattering by leaf layers with application to canopy reflectance modelling: the SAIL model. Remote Sens. Environ.,17: 125-141

ix   Atzberger C, 2004. Object-based retrieval of biophysical canopy variables using artificial neural nets and radiative transfer models. Remote Sens. Environ., 93: 53-67

x   Kuusk A, 1991. The hot spot effect in plant canopy reflectance. In: Photon-vegetation interactions: applications in optical remote sensing and plant ecology, edited by R B Myneni & J Ross (Springer, Berlin), 139-159

xi   Combal B, F Baret, M Weiss, A Trubuil, D Macé, A Pragnère, R Myneni, Y Knyazikhin and L Wang, 2002. Retrieval of canopy biophysical variables from bidirectional reflectance using prior information to solve the ill-posed inverse problem. Remote Sens. Environ., 84: 1-15

xii Jacquemoud S, F Baret, B Andrieu, F N Danson & K Jaggard, 1995. Extraction of vegetation biophysical parameters by inversion of the PROSPECT + SAIL models on sugar beet canopy reflectance data. Application to TM and AVIRIS sensors. Remote Sens. Environ., 52: 163-172

xiii Vohland M & T Jarmer. Estimating structural and biochemical parameters for grassland from spectroradiometer data by radiative transfer modelling (PROSPECT + SAIL). Int. J. Rem. Sens., in review

xiv Le Maire G, C François & E Dufrêne, 2004. Towards universal broad leaf chlorophyll indices using PROSPECT simulated database and hyperspectral reflectance measurements. Remote Sens. Environ., 89: 1-28

xv   Bacour C, S Jacquemoud, M Leroy, O Hautecœur, M Weiss, L Prévot, N Bruguier & H Chauki, 2002. Reliability of the estimation of vegetation characteristics by inversion of three canopy reflectance models on airborne POLDER data. <u>Agronomie</u>, 17: 455-464